

**PHS PUBLIC ACCESS**

Author manuscript

Sci Transl Med. Author manuscript; available in PMC 2016 April 08.

Published in final edited form as:

Sci Transl Med. 2015 August 12; 7(300): 300ra128. doi:10.1126/scitranslmed.aaa5657.**An inflammation-targeting hydrogel for local drug delivery in inflammatory bowel disease****Sufeng Zhang**^{1,2,3,*}, **Joerg Ermann**^{4,5,*}, **Marc D. Succi**^{1,2,5}, **Allen Zhou**², **Matthew J. Hamilton**^{5,6}, **Bonnie Cao**⁶, **Joshua R. Korzenik**^{5,6}, **Jonathan N. Glickman**^{5,7}, **Praveen K. Vemula**⁸, **Laurie H. Glimcher**⁹, **Giovanni Traverso**^{1,5,10,†}, **Robert Langer**^{1,3,11,†}, and **Jeffrey M. Karp**^{2,5,11,12,†}¹The David H. Koch Institute for Integrative Cancer Research, Massachusetts Institute of Technology, Cambridge, MA 02139, USA²Center for Regenerative Therapeutics, Biomedical Research Institute, Brigham and Women's Hospital, Boston, MA 02115, USA³Department of Chemical Engineering, Massachusetts Institute of Technology, Cambridge, MA 02139, USA⁴Division of Rheumatology, Immunology and Allergy, Brigham and Women's Hospital, Boston, MA 02115, USA⁵Harvard Medical School, Boston, MA 02115, USA⁶Division of Gastroenterology, Hepatology and Endoscopy, Brigham and Women's Hospital, Boston, MA 02115, USA⁷Miraca Life Sciences, Newton, MA 02464, USA⁸Institute for Stem Cell Biology and Regenerative Medicine (inStem), Bangalore 560065, India⁹Weill Cornell Medical College, New York, NY 10065, USA¹⁰Division of Gastroenterology, Massachusetts General Hospital, Boston, MA 02114, USA¹¹Harvard-Massachusetts Institute of Technology Division of Health Sciences and Technology, Cambridge, MA 02139, USA[†]Corresponding author. rlanger@mit.edu (R.L.); jmkarp@partners.org (J.M.K.); ctraverso@partners.org (GT.).

*These authors contributed equally to this work.

SUPPLEMENTARY MATERIALSwww.sciencetranslationalmedicine.org/cgi/content/full/7/300/300ra128/DC1

Methods

References (35–41)

Author contributions: S.Z. and J.E. designed and performed experiments, analyzed the data, and wrote the manuscript. M.D.S. and A.Z. assisted in performing experiments. M.J.H., B.C., and J.R.K. provided the biopsy samples from patients at the BWH Crohn's and Colitis Center. J.N.G. analyzed histology samples. P.K.V. helped analyze data and edited the manuscript. L.H.G., G.T., R.L., and J.M.K. designed experiments, supervised studies, and edited and revised the manuscript.**Competing interests**

L.H.G. has equity in and sits on the Board of Directors of Bristol-Myers Squibb. J.M.K., P.K.V., S.Z., and R.L. hold a patent related to this technology: "Nanostructured gels capable of controlled release of encapsulated agents" (U.S. Patent 20130280334 A1).

Data and materials availability

Materials are readily available and will be provided under the material transfer policies of the MIT and BWH.

¹²Harvard Stem Cell Institute, Cambridge, MA 02138, USA

Abstract

There is a clinical need for new, more effective treatments for chronic and debilitating inflammatory bowel disease (IBD), including Crohn's disease and ulcerative colitis. Targeting drugs selectively to the inflamed intestine may improve therapeutic outcomes and minimize systemic toxicity. We report the development of an inflammation-targeting hydrogel (IT-hydrogel) that acts as a drug delivery system to the inflamed colon. Hydrogel microfibers were generated from ascorbyl palmitate, an amphiphile that is generally recognized as safe (GRAS) by the U.S. Food and Drug Administration. IT-hydrogel microfibers loaded with the anti-inflammatory corticosteroid dexamethasone (Dex) were stable, released drug only upon enzymatic digestion, and demonstrated preferential adhesion to inflamed epithelial surfaces in vitro and in two mouse colitis models in vivo. Dex-loaded IT-hydrogel enemas, but not free Dex enemas, administered every other day to mice with colitis resulted in a significant reduction in inflammation and were associated with lower Dex peak serum concentrations and, thus, less systemic drug exposure. Ex vivo analysis of colon tissue samples from patients with ulcerative colitis demonstrated that IT-hydrogel microfibers adhered preferentially to mucosa from inflamed lesions compared with histologically normal sites. The IT-hydrogel drug delivery platform represents a promising approach for targeted enema-based therapies in patients with colonic IBD.

INTRODUCTION

Inflammatory bowel disease (IBD) in its two main variants, Crohn's disease and ulcerative colitis (UC), affects about 1.4 million Americans, and its incidence is increasing around the world (1, 2). Currently available therapies fail to control symptoms adequately in a significant number of patients, adversely affecting quality of life (3, 4).

One approach to develop more efficacious and safer therapies could be inflammation-targeting drug delivery to achieve high drug concentrations locally at the site of inflammation with minimal exposure of healthy or distant tissues. Enemas as a basic form of targeted drug delivery to the inflamed colon are routinely used in mild-to-moderate colitis (5). However, typical enema-based formulations require the patient to retain the enema for extended periods of time, which is difficult when suffering from diarrhea and fecal urgency. The need for frequent dosing negatively affects patient compliance (6). Furthermore, high concentrations of active drug may result in significant absorption and systemic side effects.

Inflammation targeting can potentially be achieved using drug delivery systems that exploit specific features of the diseased tissue. Inflammation of the colonic mucosa is accompanied by depletion of the mucus layer and in situ accumulation of positively charged proteins including transferrin (7), bactericidal/permeability-increasing protein, and antimicrobial peptides (8–11). This results in the buildup of positive charges at the damaged epithelial surface, providing a molecular target and anchor for drug carriers with negative surface charge (12, 13). Inflammation is furthermore accompanied by up-regulation and release of degradative enzymes including esterases and matrix metalloproteinases (MMPs) (14, 15). A drug delivery system with an overall negative surface charge and containing an enzyme-

labile linker should therefore preferentially adhere to inflamed mucosa and release drug in response to enzyme activities present at the site of inflammation. Additionally, binding of the drug carrier system to the mucosa should prolong local drug availability and permit a reduction in dosing frequency.

To identify suitable inflammation-responsive compositions, we examined hundreds of compounds from the Generally Recognized as Safe (GRAS) list of the U.S. Food and Drug Administration. Inflammation-responsive materials that have been described (16, 17) require an organic synthesis step for the introduction of MMP-labile linkers, which is complex and costly. We reasoned that the use of GRAS reagents, which are generally safe for oral consumption, inexpensive, and readily available in large quantities, should accelerate translation to the clinic. On the basis of our search for agents with enzyme-labile bonds that could be cleaved in inflammatory environments, we selected ascorbyl palmitate (AP), an amphiphile capable of self-assembly into a hydrogel in vitro (18).

We report here that a hydrogel made from AP can be used as an inflammation-targeting hydrogel (IT-hydrogel) for drug delivery in IBD (Fig. 1, A and B). IT-hydrogel microfibers encapsulate hydrophobic drugs and, owing to their negative surface charge, preferentially adhere to the inflamed mucosa in two murine colitis models, *T-bet*^{-/-}*Rag2*^{-/-}ulcerative colitis (TRUC) (19) and dextran sulfate sodium (DSS)-induced colitis, as well as to tissue samples from patients with UC. Using the corticosteroid dexamethasone (Dex) as a model drug, we demonstrate that drug-loaded IT-hydrogel microfibers administered to colitic mice via enema are therapeutically more efficacious and result in less systemic drug exposure than free Dex. Our study provides proof of concept for IT-hydrogel as a safe and potentially effective drug delivery platform for colonic IBD and other inflammatory diseases.

RESULTS

Dex is efficiently encapsulated and released from IT-hydrogel in vitro

AP consists of a partially charged hydrophilic head (ascorbic acid) and a hydrophobic tail (palmitic acid) joined by an ester bond (Fig. 1C). In a dimethyl sulfoxide (DMSO)/water solvent mixture, AP assembles into extended micellar structures and interdigitated bilayers with a hydrophobic core and hydrophilic outer layer that form fibers at the microscopic level. After heating to facilitate the dissolution of AP, gelation occurs when the AP/solvent mixture cools to room temperature (Fig. 1D).

Here, we loaded the IT-hydrogel by adding the Dex pro-drug Dex-21 palmitate (Dex-Pal) and, for imaging purposes, the fluorescent dye DiD (1,1'-dioctadecyl-3,3,3',3'-tetramethylindodicarbocyanine, 4-chlorobenzenesulfonate salt) before gelation. These hydrophobic compounds are expected to interact with the palmitic acid tails of AP and integrate into the core of the hydrogel fibers. Scanning electron microscopy revealed the fibrous structure of the IT-hydrogel with a fiber diameter of 1 to 2 μm and a length of 20 to 50 μm (Fig. 1E), which was similar for unloaded and Dex-loaded hydrogels. All IT-hydrogel formulations had a similar negative surface charge (Fig. 1F). For in vitro and in vivo applications, the IT-hydrogel was easily suspended in PBS, yielding a mixture of

microscopic fiber particles of various sizes (Fig. 1G) that could easily be handled with pipettes and syringes.

To analyze variables affecting drug encapsulation and release, Dex-loaded IT-hydrogels were generated using two concentrations of gelator [4 and 8% (w/v) AP] and two concentrations of Dex-Pal (Dex equivalent, 5 and 10 mg/ml) on the basis of our previous experience with the gels and drug-loading and delivery requirements, respectively. A lower gelator concentration (4%) and a higher Dex-Pal concentration (10 mg/ml) resulted in the best drug-loading efficiency among the formulations tested (14%, Fig. 2A). In contrast, the encapsulation efficiency was not substantially affected by the gelator and Dex-Pal concentrations (Fig. 2B).

Dex-loaded IT-hydrogel incubated in PBS at 37°C was stable for 16 days, without any measurable Dex release (Fig. 2C). Addition of an esterase, *Thermomyces lanuginosus* lipase, induced a rapid and dose-dependent release of Dex (Fig. 2C and fig. S1A). The simultaneous generation of free ascorbic acid and Dex (fig. S1, B and C) suggests that esterase hydrolyzed the ester bond in AP, causing gel disassembly while simultaneously converting Dex-Pal to active Dex by cleaving the ester bond in the palmitated pro-drug. The Dex-Pal pro-drug could not be detected in the mobile phase at any time point. Dex was more efficiently released from a 4% IT-hydrogel than from an 8% IT-hydrogel (fig. S1D).

Macrophages and other immune cells secrete enzymes at the site of inflammation that would be expected to hydrolyze the IT-hydrogel (14, 15). To simulate drug release from the IT-hydrogel under inflammatory conditions, Dex-loaded 4% IT-hydrogel microfibers were incubated in vitro with supernatant from human or mouse macrophages cultured with or without lipopolysaccharide (LPS). Enzymes secreted by both mouse and human macrophages were capable of inducing drug release from Dex-loaded IT-hydrogel (Fig. 2D). Macrophage activation by LPS enhanced the accumulation of enzymatic activity in the supernatant compared with unstimulated cells.

For subsequent in vitro and in vivo studies, we chose to use a 4% IT-hydrogel, which was less viscous than the 8% gel (fig. S1E) and thus easier to pass through syringes and small-bore tubes. We found no evidence for cytotoxicity of IT-hydrogel preparations (3 to 8% AP, \pm Dex) in two human intestinal epithelial cell lines, Caco2 and HT-29, after 72 hours in vitro (fig. S2).

IT-hydrogel preferentially adheres to inflamed mucosa in mice with colitis

The negative surface charge of the IT-hydrogel (Fig. 1F) should facilitate its adhesion to the positively charged inflamed colon epithelium (7–11). To test this hypothesis, we first analyzed the adhesive properties of IT-hydrogel microfibers in vitro using synthetic surfaces. IT-hydrogel loaded with both DiD and Dex [(DiD + Dex)/gel] was incubated on polystyrene plates coated with human recombinant transferrin (positively charged) or porcine mucin protein (negatively charged), simulating inflamed and healthy epithelium, respectively (Fig. 3A). Transferrin-coated plates retained a 7.6-fold higher fluorescence signal from the (DiD + Dex)/gel after washing compared to mucin-coated or uncoated plates (Fig. 3A). We confirmed charge interactions as the main mechanism of IT-hydrogel adhesion using

chemically defined (amine- or carboxyl-modified) substrates (fig. S3A). In another control experiment, we incubated (DiD + Dex)/gel with a cationic polyallylamine solution to convert the surface charge of the microfibers from negative to positive. As predicted, this abrogated the preferential adhesion of IT-hydrogel to transferrin and enhanced adhesion to the uncoated and mucin-coated surfaces (fig. S3B).

We then examined the adhesion of IT-hydrogel to inflamed colon epithelium using two established mouse IBD models: chemically induced DSS colitis and the spontaneous TRUC model. The distal colon was removed from mice with colitis and healthy controls, incubated with (DiD + Dex)/gel *ex vivo*, washed, and imaged using an IVIS fluorescence imaging system. Colons from wild-type mice with DSS colitis and from colitic TRUC mice showed significantly greater retention of fluorescence than colons from wild-type mice without colitis and *Rag2*^{-/-} control mice, respectively (Fig. 3B). (DiD + Dex)/gel adhered to the apical surface of the inflamed colon, as shown by confocal microscopy of frozen colon sections from a DSS mouse (fig. S4).

Preferential adhesion of IT-hydrogel to inflamed mucosa was further validated *in vivo*. Wild-type mice with DSS colitis and untreated controls, or TRUC and *Rag2*^{-/-} control mice received a single enema of (DiD + Dex)/gel. Animals were sacrificed 12 hours later, the distal colon was removed, and fluorescence retention was quantified. Colons from colitic mice demonstrated more gel adherence compared to the respective controls in both models (Fig. 3C). Administration of free DiD via enema to mice with DSS colitis did not result in retention of the fluorescence signal when the colon was analyzed 12 hours later (fig. S5). Together, these experiments provide evidence that IT-hydrogel microfibers preferentially adhere to the inflamed colon mucosa mediated by electrostatic interaction.

Drug delivery via IT-hydrogel enema improves therapeutic efficacy

We then tested IT-hydrogel in a therapeutic setting in TRUC mice. We did not examine the therapeutic efficacy of Dex-loaded IT-hydrogel in the DSS model because conflicting data about the efficacy of cortico-steroid administration on the severity of DSS colitis have been reported (20, 21). Dex was used at 70 μ g per dose on the basis of published reports of treatment studies in rodent colitis models (22, 23). Colitic TRUC mice received an enema of Dex-Pal-loaded IT-hydrogel (Dex/gel) or water-soluble Dex-21 phosphate in PBS (free Dex) on experimental days 1 and 3. Untreated mice (Control) and mice that received gel without drug (Gel) served as controls. All mice were sacrificed on day 5 for blinded histopathological analysis of the colon by a board-certified gastrointestinal pathologist (Fig. 4A). Disease severity was significantly reduced in mice given Dex/gel (mean colitis score, 1.4) compared to all other experimental groups, whereas mice in the free Dex group (mean colitis score, 3.3) did not differ significantly from untreated mice (mean colitis score, 3.4) or mice that had received gel only (mean colitis score, 4.1) (Fig. 4B). TRUC disease is characterized by infiltration of the colon lamina propria with neutrophils and mononuclear inflammatory cells, crypt hypertrophy, and superficial erosions (19, 24). Representative images (Fig. 4C) demonstrate that histological inflammation was diminished in the mice treated with two Dex/gel enemas, but not in mice receiving two enemas with the equivalent amount of free Dex. Colon weight, myeloperoxidase (MPO) activity, and expression of

tumor necrosis factor (TNF) in the distal colon were evaluated as additional parameters of disease activity in a second independent experiment (Fig. 4D). We observed a reduction of all three parameters in mice treated with Dex/gel enemas compared with the other experimental groups; the reductions of colon weight and MPO activity were statistically significant.

Although two enemas with free Dex (70 µg of Dex equivalent per dose) had no measurable effect (Fig. 4, B to D), we did observe a significant reduction in colitis severity when free Dex was administered intraperitoneally for four consecutive days (Fig. 4, E and F), demonstrating biological activity of the compound in our model. Thus, delivering Dex to colitic mice encapsulated in IT-hydrogel was significantly more efficacious than giving the equivalent amount of free Dex via enema.

We also performed an *in vivo* barrier function assay as part of the experiment reported in Fig. 4D. Treatment with two enemas of Dex/gel had no statistically significant beneficial effect on intestinal epithelial permeability compared with free Dex and control groups (fig. S6), which likely reflects both incomplete resolution of inflammation on the time scale of the experiment and the experimental noise of the assay. Longer-term and *ex vivo* studies may be needed to address this question in the future.

To demonstrate that the therapeutic benefit of Dex/gel enemas was not simply an effect of administering the pro-drug Dex-Pal, colitic TRUC mice were given two enemas of Dex-Pal suspended in a 5% ethanol/5% Tween 80 mixture on days 1 and 3, and colon histopathology was analyzed on day 5 (Fig. 4A). Administration of Dex-Pal without IT-hydrogel had no significant impact on disease severity compared with vehicle controls (Fig. 4G). These results are consistent with a model where negatively charged IT-hydrogel microfibers adhere to the inflamed colon mucosa, thereby providing a reservoir for prolonged local drug availability and improved therapeutic efficacy.

Local drug delivery via IT-hydrogel reduces systemic drug exposure

Drug release from IT-hydrogel requires enzymatic digestion of the gel by hydrolytic enzymes such as esterases (Fig. 2C) or MMPs (18). We analyzed enzyme-responsive Dex release *in vivo* by monitoring the serum drug level after administration of Dex/gel to the inflamed colon. Mice with colitis received a single enema of either Dex/gel or free Dex (70 mg of Dex equivalent in both preparations), and serum Dex levels were determined after 1, 2, 4, 6, 12, and 24 hours (Fig. 5A). Mice with DSS-induced colitis receiving free Dex had an early peak of the serum Dex concentration at 1 hour (Fig. 5B); levels declined rapidly thereafter with first-order kinetics. In mice receiving Dex/gel enemas, the peak serum concentration was significantly lower. The AUC as a measurement of cumulative systemic drug absorption was also significantly reduced in the Dex/gel mice compared with mice receiving free Dex (Fig. 5B). Similar pharmacokinetics was seen in TRUC mice (Fig. 5B). Thus, delivering Dex via IT-hydrogel altered the pharmacokinetics in both DSS colitis and TRUC models, resulting in a major reduction in systemic drug absorption.

IT-hydrogel preferentially adheres to biopsy specimens from human inflamed colon

To test the adhesion of IT-hydrogel to human colonic mucosa, we analyzed biopsy specimens from UC patients undergoing surveillance colonoscopy ($n = 6$; table S1) comparing inflamed mucosa with normal mucosa in the same patient. Freshly obtained biopsy specimens were incubated *ex vivo* with (DiD + Dex)/gel and imaged using an IVIS fluorescence imaging system (Fig. 6A). Specimens from inflamed sites retained significantly more fluorescence than did those from normal sites (Fig. 6, B and C); the mean fold difference between inflamed and normal biopsy specimens was 5.4. The *ex vivo* analysis of human biopsy samples therefore demonstrates, consistent with our mouse data, that IT-hydrogel microfibers preferentially adhere to inflamed mucosa in patients with active UC.

DISCUSSION

Drug therapy involves the careful balancing of intended therapeutic effects and unwanted side effects often related to activities in organs not affected by the disease. One approach to maximize beneficial effects and reduce the potential for side effects is targeted drug delivery and release. Many oral formulations for drug delivery to the colon rely on pH-, time-, microflora-, or pressure-triggered mechanisms and target the intestinal region rather than the inflamed intestine (25). In contrast, inflammation-targeting drug delivery systems use specific features of the inflamed target organ. Poly(lactic-*co*-glycolic acid) nanoparticles have been shown to accumulate in the inflamed mucosa after oral administration to rats with trinitrobenzenesulfonic acid-induced colitis owing to increased tissue permeability at the site of inflammation (26), and poly(thioketal) nanoparticles release drug upon degradation by reactive oxygen species present in the colon of mice with DSS-induced colitis (27). The inflamed intestine has also been targeted from the bloodstream using PEGylated poly(lactic acid) microparticles coated with antibodies against an endothelial cell adhesion molecule up-regulated in mouse colitis models (28, 29).

Here, we demonstrate that IT-hydrogel fibers with a negatively charged surface preferentially adhere to positively charged artificial surfaces, to inflamed mucosa in murine colitis, and to biopsy specimens from inflamed colon mucosa in human UC patients. Although we cannot exclude the possibility that additional factors may play a role *in vivo*, our *in vitro* data strongly suggest charge as the main factor mediating adhesion of IT-hydrogel to the inflamed epithelial surface. This is consistent with published reports describing the use of anionic liposomes for drug delivery to the inflamed intestine (12, 13). We were able to detect a fluorescence signal from the intestinal wall for at least 12 hours after administration of a single enema of fluorescently labeled IT-hydrogel to mice with colitis. This suggests that adherent IT-hydrogel microfibers generate a reservoir of encapsulated drug at the site of inflammation, thereby prolonging local drug availability. Drug delivery using IT-hydrogel enemas may thus allow for less frequent dosing in patients with IBD.

Compared with other drug delivery systems targeting the inflamed colon mucosa, IT-hydrogel has several potential advantages. First, the IT-hydrogel described here is made from a nontoxic, GRAS compound (30), which should facilitate rapid translation into the clinic. Many GRAS agents are relatively inexpensive and available in large quantities at a

high grade of purity (Good Manufacturing Practice or Food Grade). Second, the gelation process for the IT-hydrogel is simple and easy to scale up. Third, IT-hydrogel has a high drug-loading capacity, owing to the small molecular weight of the gelator and the availability of all gelator molecules to form intermolecular interactions. Fourth, drug-loaded IT-hydrogel exhibits long-term stability, which enables sustained drug release over several days. Presumably, the microstructure of the gel fibers protects the ester bond between ascorbic acid and palmitic acid from spontaneous hydrolysis by water, because water cannot efficiently penetrate into the hydrophobic fiber core to disassemble the gel and release the drug. Drug release requires hydrolytic enzyme activities, which are up-regulated at sites of inflammation, further strengthening the inflammation-responsive aspect of this system.

IT-hydrogel microfibers made from AP are representative of a first generation of inflammation-targeting drug delivery systems prepared from amphiphile GRAS reagents. Potential applications are not limited to IBD but include any disease where controlled drug release at a distinct location is desired. We recently reported that delivery of an immunosuppressive drug (tacrolimus) using an enzyme-responsive hydrogel prepared from another GRAS reagent (triglycerol monostearate) improved long-term survival of vascularized allografts in rats (31). In that study, the drug-loaded hydrogel was injected subcutaneously into the allograft. Here, we used topical enzyme-responsive drug release in combination with inflammation-sensitive charge-based adhesion to improve drug delivery to the inflamed colon.

To analyze gel adhesion and drug delivery via IT-hydrogel *in vivo*, we used two mouse IBD models, TRUC and DSS-induced colitis models. In both models, we found preferential adhesion of IT-hydrogel to the inflamed mucosa and reduced systemic drug absorption after enema administration of Dex-loaded IT-hydrogel compared with free Dex. We could demonstrate that IT-hydrogel also adhered significantly better to biopsy specimens from inflamed mucosal locations in patients with UC compared with specimens from normal sites. All patients were on anti-inflammatory medications at the time of biopsy; our results may therefore underestimate the binding efficacy of the IT-hydrogel to the inflamed mucosa in untreated patients.

We loaded IT-hydrogel microfibers with the corticosteroid Dex to examine the utility of this system for inflammation-targeting drug delivery in mice *in vivo*. Delivering Dex encapsulated in IT-hydrogel reduced systemic absorption compared with free Dex administered via enema and improved its therapeutic efficacy in the TRUC model. We analyzed only one drug (Dex) whose anti-inflammatory properties are well described (32, 33). However, the investigation of novel drug targets was not the focus of our study. Rather, we consider Dex as a model drug to demonstrate the utility of the IT-hydrogel in colonic IBD. Our approach could potentially be applied to many other drugs, including small-molecule inhibitors of signaling cascades (31).

We did not achieve complete resolution of colon inflammation by giving TRUC mice two Dex/gel enemas (Fig. 4, B to D, and fig. S6). However, we chose a treatment regimen that might discern a difference in therapeutic response between Dex/gel and free Dex considering that free Dex effectively treats TRUC when administered in high enough

quantities (Fig. 4F). Long-term experiments with more stringent end points including assays of intestinal barrier function will be important when testing future IT-hydrogel formulations. The use of a single mouse model for the analysis of therapeutic efficacy is another potential limitation of our study. Additional preclinical studies including large animal models are needed before the clinical benefits of IT-hydrogel can be evaluated in humans.

In conclusion, we have developed a strategy for targeted drug delivery to the inflamed colonic mucosa using hydrogel microfibers prepared from an amphiphilic GRAS reagent. Through attaching to the inflamed mucosa and selectively releasing drug at the site of inflammation, this system has the potential to prolong local drug availability, minimize systemic drug absorption, reduce dosing frequency, and lower the burden on the patient for retaining enemas after administration, all of which should improve compliance, reduce the risk for systemic toxicity, and maximize therapeutic efficacy.

MATERIALS AND METHODS

Study design

The goal of this study was to engineer an inflammation-targeting drug delivery system (IT-hydrogel) for IBD of the colon. We hypothesized that negatively charged IT-hydrogel microfibers should rapidly adhere to inflamed colon mucosa and selectively release their drug cargo upon enzymatic digestion. After characterization of the IT-hydrogel *in vitro*, we examined whether drug delivery via IT-hydrogel enemas would affect therapeutic efficacy and systemic drug absorption in two mouse models of IBD, DSS-induced colitis and the spontaneous TRUC model. Throughout this study, the anti-inflammatory drug Dex was used as a model drug—either the hydrophobic pro-drug Dex-Pal for loading into IT-hydrogel microfibers or the water-soluble Dex-21 phosphate. Animals were randomly assigned to different treatment groups. DSS-treated animals without weight loss were excluded from the study before randomization. For imaging experiments, 5 to 7 mice were used per group; for treatment and pharmacokinetic studies, we used 7 to 10 mice per group on the basis of previous studies. All animals were included in the analysis. Histopathology was analyzed by an experienced gastrointestinal pathologist (J.N.G.) blinded to group assignment using an established scoring system. Adhesion of IT-hydrogel to human colon mucosa was tested using biopsy specimens from patients with UC. Patients were from the Brigham and Women's Hospital (BWH) Crohn's and Colitis Center who had given informed consent to collect biopsy specimens for research purposes under a protocol approved by the Institutional Review Board of Partners HealthCare.

Mice

TRUC (*T-bet*^{-/-}*Rag2*^{-/-}) (19) and *Rag2*^{-/-} lines on a BALB/c genetic background were maintained in a specific pathogen-free animal facility at the Harvard School of Public Health (HSPH). The mice were housed in microisolator cages with Sulfatrim [sulfamethoxazole (1 g/liter) + trimethoprim (0.2 g/liter); Hi-Tech Pharmacal] added to the drinking water. TRUC and *Rag2*^{-/-} mice were used for experiments at 8 to 10 weeks of age. Adult BALB/c wild-type mice were purchased from the Jackson Laboratory. Experiments involving wild-type mice were performed either at HSPH or at the David H. Koch Institute for Integrative

Cancer Research at Massachusetts Institute of Technology (MIT). All mouse studies were performed according to institutional and National Institutes of Health (NIH) guidelines for humane animal use. Experimental protocols were approved by the Animal Care Committees at Harvard University and MIT.

Preparation of IT-hydrogel

IT-hydrogel (3 to 8%, w/v) was prepared using DMSO (Sigma-Aldrich) and H₂O as a solvent pair (volume ratio, DMSO/H₂O = 1:4). After dissolving AP (Sigma-Aldrich) in DMSO, H₂O was added dropwise. The vial was heated to 60° to 80°C until AP was completely dissolved and then allowed to cool down to room temperature (18). The formed hydrogel was washed with PBS and centrifuged at 6000 rpm for 10 min (3×). For preparation of sterile hydrogels, all solutions were sterilized before gelation using 0.20-μm syringe filters. Hydrogel morphology was characterized by environmental scanning electron microscopy (FEI/Philips XL30 FEG, 1000×, acceleration voltage, 10.0 kV). The washed hydrogel pellet was suspended in PBS for polarized optical microscopy imaging (Zeiss Axioplan2, 40×).

Dex encapsulation

Dex-Pal (Toronto Research Chemicals Inc.) was mixed with AP in DMSO before adding H₂O. To quantify the drug-loading efficiency (weight of incorporated drug divided by weight of drug-loaded gel) and encapsulation efficiency (weight of incorporated drug divided by weight of input drug), the hydrogel pellet was lyophilized and dissolved in DMSO for high-performance liquid chromatography (HPLC) analysis.

Cell culture

Primary macrophages were generated by injecting wild-type BALB/c mice with 2.5 ml of 3% thioglycolate (BD Biosciences) intraperitoneally. Peritoneal cells were harvested on day 3 by lavage with ice-cold PBS. Cells (1.5×10^6) were plated in 3 ml of RPMI 1640 (Cellgro) supplemented with 10% fetal calf serum (Atlanta Biologicals), 10 mM HEPES, 1 mM sodium pyruvate, 2 mM L-glutamine, penicillin (100 U/ml), streptomycin (100 μg/ml) (all Cellgro), and 50 μM β-mercaptoethanol (Sigma-Aldrich) (RPMI-C). The cells were allowed to adhere overnight. They were then stimulated with LPS (*Escherichia coli* 0111:B4, Sigma-Aldrich) at 1 μg/ml. Supernatant was harvested after 24, 48, and 72 hours. THP-1 cells (American Type Culture Collection) were cultured in RPMI-C. For differentiation into macrophages, 1.25×10^6 cells were seeded on six-well plates in 2.5 ml of RPMI-C plus 50 nM phorbol 12-myristate 13-acetate 3 days before stimulation. Medium was changed to fresh medium 1 day before stimulation with LPS (100 ng/ml). Supernatant was harvested after 4 and 24 hours and frozen at -80°C until analysis.

Ex vivo and in vivo gel adhesion experiments

Animals with colitis (TRUC or DSS) and disease-free controls (*Rag2*^{-/-} or untreated wild type, respectively) were on an alfalfa-free diet (Harlan Laboratories) for 1 week before experiments. For ex vivo adhesion testing, the most distal 1.5 cm of colon tissue excluding the anus was dissected. Two hundred microliters of (DiD + Dex)-loaded 4% IT-hydrogel

[(DiD + Dex)/gel] was suspended in 6 ml of PBS. The colon was inverted and incubated in 0.5 ml of gel suspension for 30 min at 37°C with gentle shaking (34). After washing with PBS (3×), the colon was opened longitudinally and imaged using an IVIS fluorescence imager (IVIS 200, PerkinElmer) with the luminal side facing up.

For *in vivo* adhesion testing, animals were fasted overnight, and the following morning, each mouse received an enema of 100 µl (DiD + Dex)/gel. Individual mice were anesthetized with 2.5% isoflurane, a 20-gauge flexible disposable feeding needle (Braintree Scientific) was advanced into the rectum 3 cm past the anus, (DiD + Dex)/gel was administered, the catheter was removed, and the anus was kept closed manually for 1 min. Animals were sacrificed after 12 hours. The distal 3 cm of the colon was removed and imaged freshly without washing. The fluorescence signal intensity was quantified using Living Image software (version 4.3.1, PerkinElmer) in a standard-size ROI drawn around individual colon pieces. Background fluorescence intensity determined as the average of three ROIs not containing any colon tissue was subtracted from all specimens.

In vivo treatment of established colitis

TRUC mice were randomized to one of four experimental groups: (i) control (no treatment or 100 µl of PBS enema), (ii) gel enema (4% IT-hydrogel suspended in 100 µl of PBS), (iii) free Dex enema (Dex-21 phosphate in 100 µl of PBS, 70 µg of Dex equivalent), and (iv) Dex/gel enema (Dex-Pal in 4% IT-hydrogel suspended in 100µl of PBS, 70 µg of Dex equivalent). Enemas were administered on days 1 and 3 after fasting the mice overnight as described. Duplicate aliquots of the enema suspension or solution given to the mice in groups iii and iv were analyzed by HPLC to confirm the Dex equivalent content in Dex-Pal or Dex-21 phosphate.

In one control experiment (Fig. 4F), TRUC mice received four daily consecutive intraperitoneal injections of free Dex (70 µg of Dex equivalent) or PBS alone. In a second control experiment (Fig. 4G), TRUC mice received enemas on days 1 and 3 of Dex-Pal (70 µg of Dex equivalent) dissolved in 100 µl of 5% ethanol + 5% Tween 80 (Sigma-Aldrich) or carrier alone.

All mice were sacrificed for histopathological analysis on day 5. Colons were isolated, fixed in 4% paraformaldehyde, and embedded in paraffin. Standard H&E-stained sections were examined and scored by an experienced pathologist (J.N.G.) in a blinded fashion. Mononuclear cell infiltration, polymorphonuclear cell infiltration, epithelial hyperplasia, and epithelial injury are the four components in the score that were independently graded as absent (0), mild (1), moderate (2), or severe (3), giving a total score of 0 to 12 (19, 24).

Ex vivo gel adhesion experiments with colon biopsy specimens from patients with UC

Two biopsies from inflamed and normal mucosa as evaluated endoscopically were taken from each patient, placed immediately in PBS, and transported on ice to the laboratory. A third biopsy from each site was sent to the clinical pathology laboratory for routine histopathology evaluation. The adhesion test was performed within 4 hours of the biopsy as follows. Two hundred microliters of (DiD + Dex)-loaded 4% IT-hydrogel was suspended in 6 ml of PBS. Individual specimens were incubated in 0.5 ml of the gel suspension for 30

min at 37°C with gentle shaking. After washing with PBS (3×), the samples were placed on a black plastic sheet and imaged using an IVIS fluorescence imager (IVIS 200, PerkinElmer). Fluorescence signal intensity was quantified using the Living Image software (version 4.3.1, PerkinElmer). The specimens were subsequently air-dried and weighed to determine the weight-normalized fluorescence signal intensity. Specimens from 11 patients (table S1) were assayed. For inclusion in the analysis (Fig. 6), we required that endoscopy and histopathology reports were concordant for either “normal” or “inflamed” mucosa; for this reason, four patients were excluded; a fifth patient was excluded because the inflamed specimen was derived from the appendiceal orifice (table S1).

Statistical analysis

The two-tailed Student’s *t* test was used to compare differences between two experimental groups, except for the study with UC patients where the paired *t* test was used. In experiments with multiple groups, one-way ANOVA with Tukey post hoc test was used. A value of $P < 0.05$ was considered statistically significant. Statistical analysis and graphing were performed with Prism 6 (GraphPad Software).

Supplementary Material

Refer to Web version on PubMed Central for supplementary material.

Acknowledgments

We thank S. Malstrom for advice on IVIS imaging setup and data analysis, W. Salmon for assistance with polarized light microscopy and the confocal microscopy, J. Ramirez for expert animal care, Q. Wang for help with the rheological assay, D. Huang for help with the in vitro adhesion assay, and M. Ma and N. Bertrand for helpful discussions.

Funding: S.Z. received a fellowship from the Natural Sciences and Engineering Research Council of Canada. P.K.V. received a Ramalingaswami Re-entry Fellowship from the Department of Biotechnology, India. This work was supported by Harvard Institute of Translational Immunology/Helmley Trust Pilot Grants in Crohn’s Disease to J.E., L.H.G., and J.M.K.; NIH grant CA112663 to L.H.G.; NIH grant T32DK7191-38-S1 to G.T.; NIH grants DE013023 and EB000244 and a Max Planck Research Award from the Alexander von Humboldt Foundation to R.L.; and NIH grants DE023432 and AR063866 to J.M.K.

REFERENCES AND NOTES

- Loftus EV Jr. Clinical epidemiology of inflammatory bowel disease: Incidence, prevalence, and environmental influences. *Gastroenterology*. 2004; 126:1504–1517. [PubMed: 15168363]
- Molodecky NA, Soon IS, Rabi DM, Ghali WA, Ferris M, Chernoff G, Benchimol EI, Panaccione R, Ghosh S, Barkema HW, Kaplan GG. Increasing incidence and prevalence of the inflammatory bowel diseases with time, based on systematic review. *Gastroenterology*. 2012; 142:46–54.e42. [PubMed: 22001864]
- Hoivik ML, Moum B, Solberg IC, Cvancarova M, Hoie O, Vatn MH, Bernklev T. IBSEN Study Group, Health-related quality of life in patients with ulcerative colitis after a 10-year disease course: Results from the IBSEN study. *Inflamm Bowel Dis*. 2012; 18:1540–1549. [PubMed: 21936030]
- Ghosh S, Mitchell R. Impact of inflammatory bowel disease on quality of life: Results of the European Federation of Crohn’s and Ulcerative Colitis Associations (EFCCA) patient survey. *J Crohns Colitis*. 2007; 1:10–20. [PubMed: 21172179]
- Kornbluth A, Sachar DB. Practice Parameters Committee of the American College of Gastroenterology, Ulcerative colitis practice guidelines in adults: American College of Gastroenterology. *Gastroenterology*. 2010; 138:1569–1590. [PubMed: 20514040]

- ogy, Practice Parameters Committee. *Am J Gastroenterol.* 2010; 105:501–523. [PubMed: 20068560]
6. Ediger JP, Walker JR, Graff L, Lix L, Clara I, Rawsthorne P, Rogala L, Miller N, McPhail C, Deering K, Bernstein CN. Predictors of medication adherence in inflammatory bowel disease. *Am J Gastroenterol.* 2007; 102:1417–1426. [PubMed: 17437505]
 7. Tirosch B, Khatib N, Barenholz Y, Nissan A, Rubinstein A. Transferrin as a luminal target for negatively charged liposomes in the inflamed colonic mucosa. *Mol Pharm.* 2009; 6:1083–1091. [PubMed: 19603812]
 8. Canny G, Levy O, Furuta GT, Narravula-Alipati S, Sisson RB, Serhan CN, Colgan SP. Lipid mediator-induced expression of bactericidal/permeability-increasing protein (BPI) in human mucosal epithelia. *Proc Natl Acad Sci USA.* 2002; 99:3902–3907. [PubMed: 11891303]
 9. Monajemi H, Meenan J, Lamping R, Obradov DO, Radema SA, Trown PW, Tytgat GN, Van Deventer SJ. Inflammatory bowel disease is associated with increased mucosal levels of bactericidal/permeability-increasing protein. *Gastroenterology.* 1996; 110:733–739. [PubMed: 8608882]
 10. Ramasundara M, Leach ST, Lemberg DA, Day AS. Defensins and inflammation: The role of defensins in inflammatory bowel disease. *J Gastroenterol Hepatol.* 2009; 24:202–208. [PubMed: 19215333]
 11. Wehkamp J, Fellermann K, Herrlinger KR, Baxmann S, Schmidt K, Schwind B, Duchrow M, Wohlschläger C, Feller AC, Stange EF. Human β -defensin 2 but not β -defensin 1 is expressed preferentially in colonic mucosa of inflammatory bowel disease. *Eur J Gastroenterol Hepatol.* 2002; 14:745–752. [PubMed: 12169983]
 12. Jubeh TT, Barenholz Y, Rubinstein A. Differential adhesion of normal and inflamed rat colonic mucosa by charged liposomes. *Pharm Res.* 2004; 21:447–453. [PubMed: 15070095]
 13. Jubeh TT, Nadler-Milbauer M, Barenholz Y, Rubinstein A. Local treatment of experimental colitis in the rat by negatively charged liposomes of catalase, TMN and SOD. *J Drug Target.* 2006; 14:155–163. [PubMed: 16753829]
 14. Wiener E, Levanon D. Macrophage cultures: An extracellular esterase. *Science.* 1968; 159:217. [PubMed: 5634918]
 15. Sorokin L. The impact of the extracellular matrix on inflammation. *Nat Rev Immunol.* 2010; 10:712–723. [PubMed: 20865019]
 16. Lutolf MP, Lauer-Fields JL, Schmoekel HG, Metters AT, Weber FE, Fields GB, Hubbell JA. Synthetic matrix metalloproteinase-sensitive hydrogels for the conduction of tissue regeneration: Engineering cell-invasion characteristics. *Proc Natl Acad Sci USA.* 2003; 100:5413–5418. [PubMed: 12686696]
 17. Patterson J, Hubbell JA. Enhanced proteolytic degradation of molecularly engineered PEG hydrogels in response to MMP-1 and MMP-2. *Biomaterials.* 2010; 31:7836–7845. [PubMed: 20667588]
 18. Vemula PK, Boilard E, Syed A, Campbell NR, Muluneh M, Weitz DA, Lee DM, Karp JM. On-demand drug delivery from self-assembled nanofibrous gels: A new approach for treatment of proteolytic disease. *J Biomed Mater Res A.* 2011; 97:103–110. [PubMed: 21404422]
 19. Garrett WS, Lord GM, Punit S, Lugo-Villarino G, Mazmanian SK, Ito S, Glickman JN, Glimcher LH. Communicable ulcerative colitis induced by T-bet deficiency in the innate immune system. *Cell.* 2007; 131:33–45. [PubMed: 17923086]
 20. van Meeteren ME, Meijssen MA, Zijlstra FJ. The effect of dexamethasone treatment on murine colitis. *Scand. J Gastroenterol.* 2000; 35:517–521.
 21. Kojouharoff G, Hans W, Obermeier F, Männel DN, Andus T, Schölmerich J, Gross V, Falk W. Neutralization of tumour necrosis factor (TNF) but not of IL-1 reduces inflammation in chronic dextran sulphate sodium-induced colitis in mice. *Clin Exp Immunol.* 1997; 107:353–358. [PubMed: 9030875]
 22. Yuan H, Ji WS, Wu KX, Jiao JX, Sun LH, Feng YT. Anti-inflammatory effect of Diammonium Glycyrrhizinate in a rat model of ulcerative colitis. *World J Gastroenterol.* 2006; 12:4578–4581. [PubMed: 16874877]

23. Cannarile L, Cuzzocrea S, Santucci L, Agostini M, Mazzon E, Esposito E, Muià C, Coppo M, Di Paola R, Riccardi C. Glucocorticoid-induced leucine zipper is protective in Th1-mediated models of colitis. *Gastroenterology*. 2009; 136:530–541. [PubMed: 18996377]
24. Ermann J, Staton T, Glickman JN, de Waal Malefyt R, Glimcher LH. Nod/Ripk2 signaling in dendritic cells activates IL-17A-secreting innate lymphoid cells and drives colitis in *Tbet^{-/-}Rag2^{-/-}* (TRUC) mice. *Proc Natl Acad Sci USA*. 2014; 111:E2559–E2566. [PubMed: 24927559]
25. Dahan A, Amidon GL, Zimmermann EM. Drug targeting strategies for the treatment of inflammatory bowel disease: A mechanistic update. *Expert Rev Clin Immunol*. 2010; 6:543–550. [PubMed: 20594127]
26. Lamprecht A, Ubrich N, Yamamoto H, Schäfer U, Takeuchi H, Maincent P, Kawashima Y, Lehr CM. Biodegradable nanoparticles for targeted drug delivery in treatment of inflammatory bowel disease. *J Pharmacol Exp Ther*. 2001; 299:775–781. [PubMed: 11602694]
27. Wilson DS, Dalmasso G, Wang L, Sitaraman SV, Merlin D, Murthy N. Orally delivered thioketal nanoparticles loaded with TNF- α -siRNA target inflammation and inhibit gene expression in the intestines. *Nat Mater*. 2010; 9:923–928. [PubMed: 20935658]
28. Sakhalkar HS, Dalal MK, Salem AK, Ansari R, Fu J, Kiani MF, Kurjiaka DT, Hanes J, Shakesheff KM, Goetz DJ. Leukocyte-inspired biodegradable particles that selectively and avidly adhere to inflamed endothelium in vitro and in vivo. *Proc Natl Acad Sci USA*. 2003; 100:15895–15900. [PubMed: 14668435]
29. Sakhalkar HS, Hanes J, Fu J, Benavides U, Malgor R, Borruso CL, Kohn LD, Kurjiaka DT, Goetz DJ. Enhanced adhesion of ligand-conjugated biodegradable particles to colitic venules. *FASEB J*. 2005; 19:792–794. [PubMed: 15764649]
30. Food and Drug Administration. Generally Recognized as Safe (GRAS). www.fda.gov/Food/IngredientsPackagingLabeling/GRAS/
31. Gajanayake T, Olariu R, Leclère FM, Dhayani A, Yang Z, Bongoni AK, Banz Y, Constantinescu MA, Karp JM, Vemula PK, Rieben R, Vögelin E. A single localized dose of enzyme-responsive hydrogel improves long-term survival of a vascularized composite allograft. *Sci Transl Med*. 2014; 6:249ra110.
32. Stahn C, Löwenberg M, Hommes DW, Buttgerit F. Molecular mechanisms of glucocorticoid action and selective glucocorticoid receptor agonists. *Mol Cell Endocrinol*. 2007; 275:71–78. [PubMed: 17630118]
33. Tsurufuji S, Sugio K, Takemasa F. The role of glucocorticoid receptor and gene expression in the anti-inflammatory action of dexamethasone. *Nature*. 1979; 280:408–410. [PubMed: 460415]
34. Harel E, Rubinstein A, Nissan A, Khazanov E, Milbauer MNadler, Barenholz Y, Tirosh B. Enhanced transferrin receptor expression by proinflammatory cytokines in enterocytes as a means for local delivery of drugs to inflamed gut mucosa. *PLOS One*. 2011; 6:e24202. [PubMed: 21915296]
35. Li F, Hui DY. Modified low density lipoprotein enhances the secretion of bile salt-stimulated cholesterol esterase by human monocyte-macrophages. Species-specific difference in macrophage cholesteryl ester hydrolase. *J Biol Chem*. 1997; 272:28666–28671. [PubMed: 9353334]
36. Lu X, Howard MD, Mazik M, Eldridge J, Rinehart JJ, Jay M, Leggas M. Nanoparticles containing anti-inflammatory agents as chemotherapy adjuvants: Optimization and in vitro characterization. *AAPS J*. 2008; 10:133–140. [PubMed: 18446513]
37. Higai K, Ichikawa A, Matsumoto K. Binding of sialyl Lewis X antigen to lectin-like receptors on NK cells induces cytotoxicity and tyrosine phosphorylation of a 17-kDa protein. *Biochim. Biophys Acta*. 2006; 1760:1355–1363.
38. Svensson O, Thuresson K, Arnebrant T. Interactions between chitosan-modified particles and mucin-coated surfaces. *J Colloid Interface Sci*. 2008; 325:346–350. [PubMed: 18597767]
39. Jang WS, Jensen AT, Lutkenhaus JL. Confinement effects on cross-linking within electrostatic layer-by-layer assemblies containing poly(allylamine hydrochloride) and poly(acrylic acid). *Macromolecules*. 2010; 43:9473–9479.

40. Yan Y, Kolachala V, Dalmasso G, Nguyen H, Laroui H, Sitaraman SV, Merlin D. Temporal and spatial analysis of clinical and molecular parameters in dextran sodium sulfate induced colitis. *PLOS One*. 2009; 4:e6073. [PubMed: 19562033]
41. Bradley PP, Priebat DA, Christensen RD, Rothstein G. Measurement of cutaneous inflammation: Estimation of neutrophil content with an enzyme marker. *J Invest Dermatol*. 1982; 78:206–209. [PubMed: 6276474]

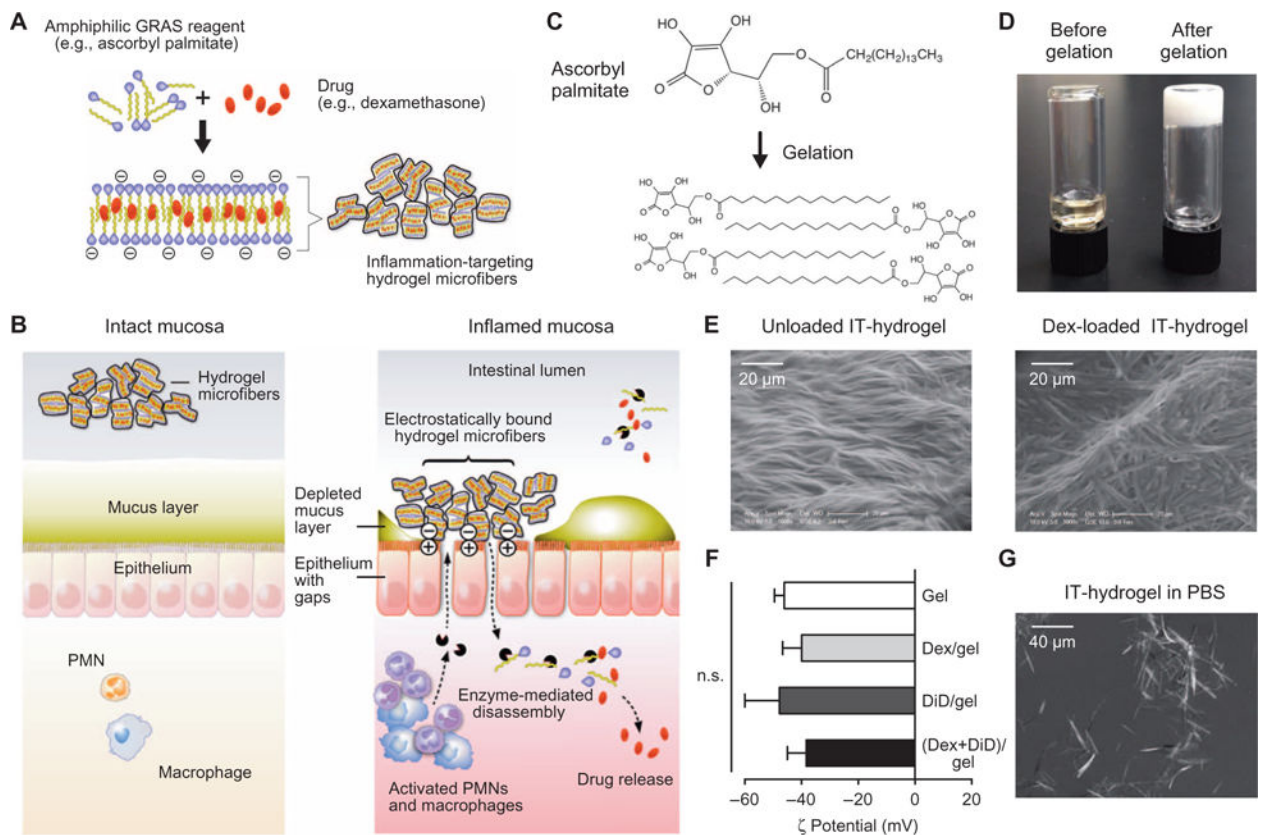


Fig. 1. IT-hydrogel targets drug release to the inflamed mucosa

(A) A lipophilic drug is loaded into IT-hydrogel during gelation. The drug integrates into the hydrophobic core of the lipid bilayer. Microfibers represent higher-order assemblies of extended bilayer structures, which are suspended in phosphate-buffered saline (PBS) to yield a mixture of microscopic hydrogel fiber particles of various sizes. (B) Negatively charged IT-hydrogel microfibers do not adhere to the intact mucosal surface. The inflamed mucosa is characterized by mucus depletion, accumulation of positively charged proteins, and increased permeability of the epithelial cell layer. Negatively charged IT-hydrogel microfibers adhere to the positively charged inflamed epithelium. Hydrolytic enzymes released by inflammatory cells degrade the gel, resulting in drug release. PMN, polymorphonuclear leukocytes. (C) Molecular structure of AP (top) and the assembled IT-hydrogel (bottom) demonstrating the alignment of the hydrophobic tails in the center and the hydrophilic heads on the outside of the bilayer. (D) AP before and after gelation. (E) Environmental scanning electron microscopy images of unloaded and Dex-loaded IT-hydrogel before suspension in PBS. (F) ζ Potential of IT-hydrogel (Gel) or gel loaded with Dex (Dex/gel), DiD (DiD/gel), or Dex+DiD [(Dex+DiD)/gel]. Data are means ± SD ($n=6$ pooled from two experiments); $P=0.1485$ determined by one-way analysis of variance (ANOVA). (G) Polarized optical microscopy image of IT-hydrogel suspended in PBS.

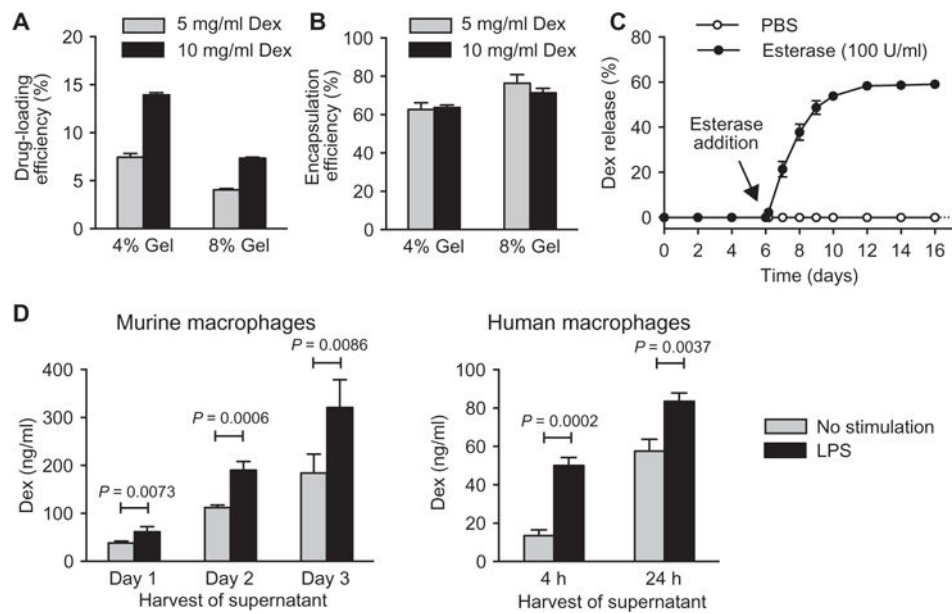


Fig. 2. Dex is efficiently encapsulated into IT-hydrogel and released by esterase activity and supernatant from macrophages

(A and B) Drug-loading and encapsulation efficiencies for 4 and 8% AP gelator with Dex-Pal at Dex equivalent of 5 and 10 mg/ml. (C) Esterase-responsive Dex release from IT-hydrogel. Esterase (*T. lanuginosus* lipase, 100 U/ml) was added on day 6. (D) Dex release from IT-hydrogel upon incubation with culture supernatant from activated mouse or human macrophages for 24 hours at 37°C. The 4% IT-hydrogel (C) and (D) was loaded with Dex-Pal (Dex equivalent, 5 mg/ml). Data are means \pm SD ($n = 3$, performed at least twice); P values in (D) were determined by Student's t test with the Holm-Sidak method to correct for multiple comparisons.

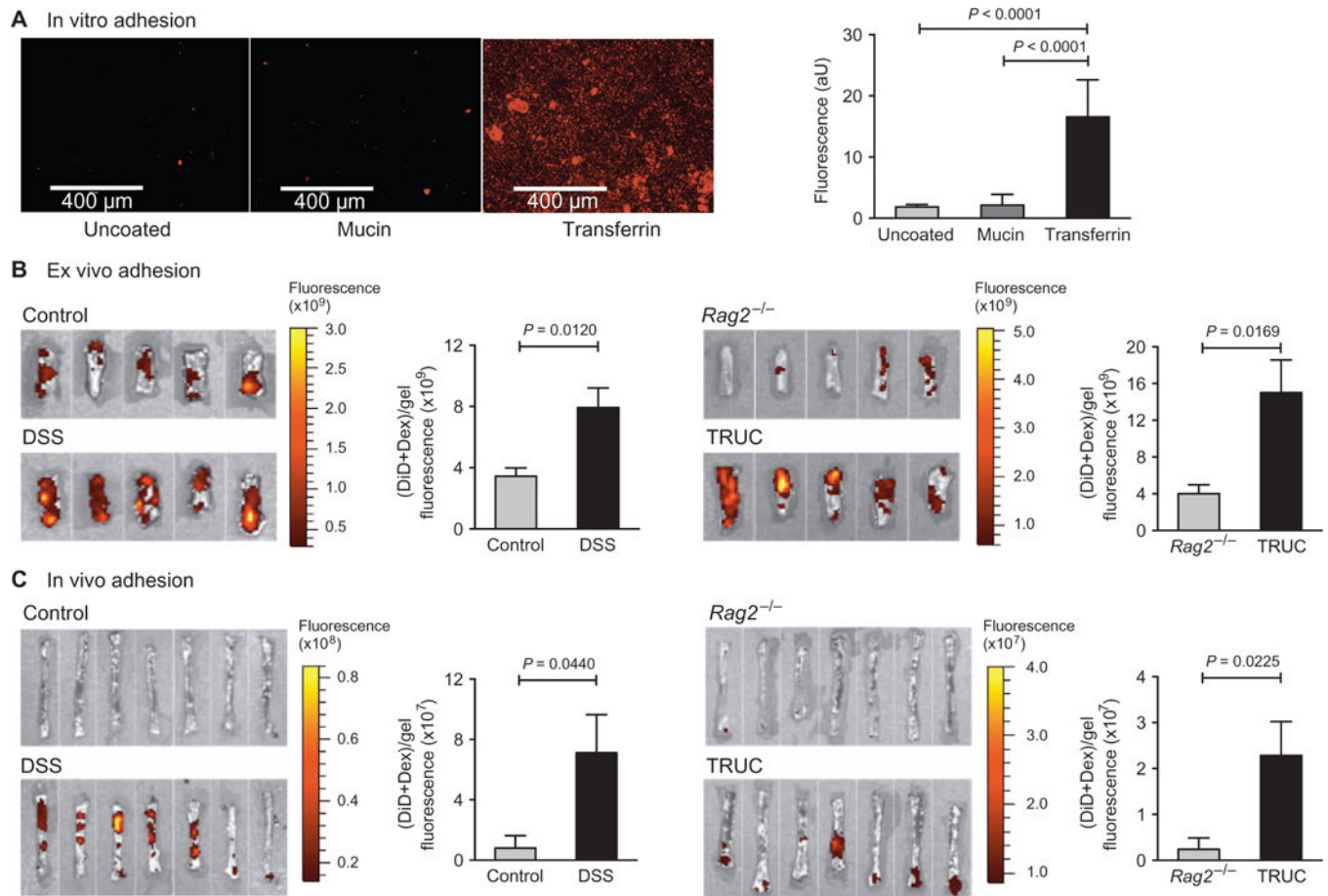


Fig. 3. IT-hydrogel preferentially adheres to inflamed mucosa

(A) (DiD + Dex)-loaded 4% IT-hydrogel [(DiD + Dex)/gel] was incubated with uncoated, mucin-coated (simulating healthy epithelium), or transferrin-coated (simulating inflamed epithelium) surfaces at 37°C for 1 hour. Fluorescence images obtained after rinsing (left) were quantified using ImageJ software (right). Data are means \pm SD ($n = 9$, triplicate samples, three images per sample); P values were determined by one-way ANOVA with Tukey post hoc test. aU, arbitrary unit. (B) The distal colon of wild-type (WT) mice with DSS-induced colitis and healthy controls was incubated ex vivo with (DiD+Dex)/gel at 37°C for 30 min and washed, and fluorescence was quantified using an IVIS imaging system (left). The same experimental setup compared colitic TRUC mice and age-matched *Rag2*^{-/-} mice without colitis (right). (C) WT mice with DSS-induced colitis and healthy controls received an enema of (DiD + Dex)/gel. The animals were sacrificed 12 hours later, and fluorescence of the distal colon was measured (left). The same experimental setup compared colitic TRUC and control *Rag2*^{-/-} mice (right). In (B) and (C), the total fluorescence intensity was determined in a standard-size region of interest (ROI) drawn around the individual colon pieces; data are means \pm SEM ($n = 5$ to 7 mice per group); P values were determined by Student's t test.

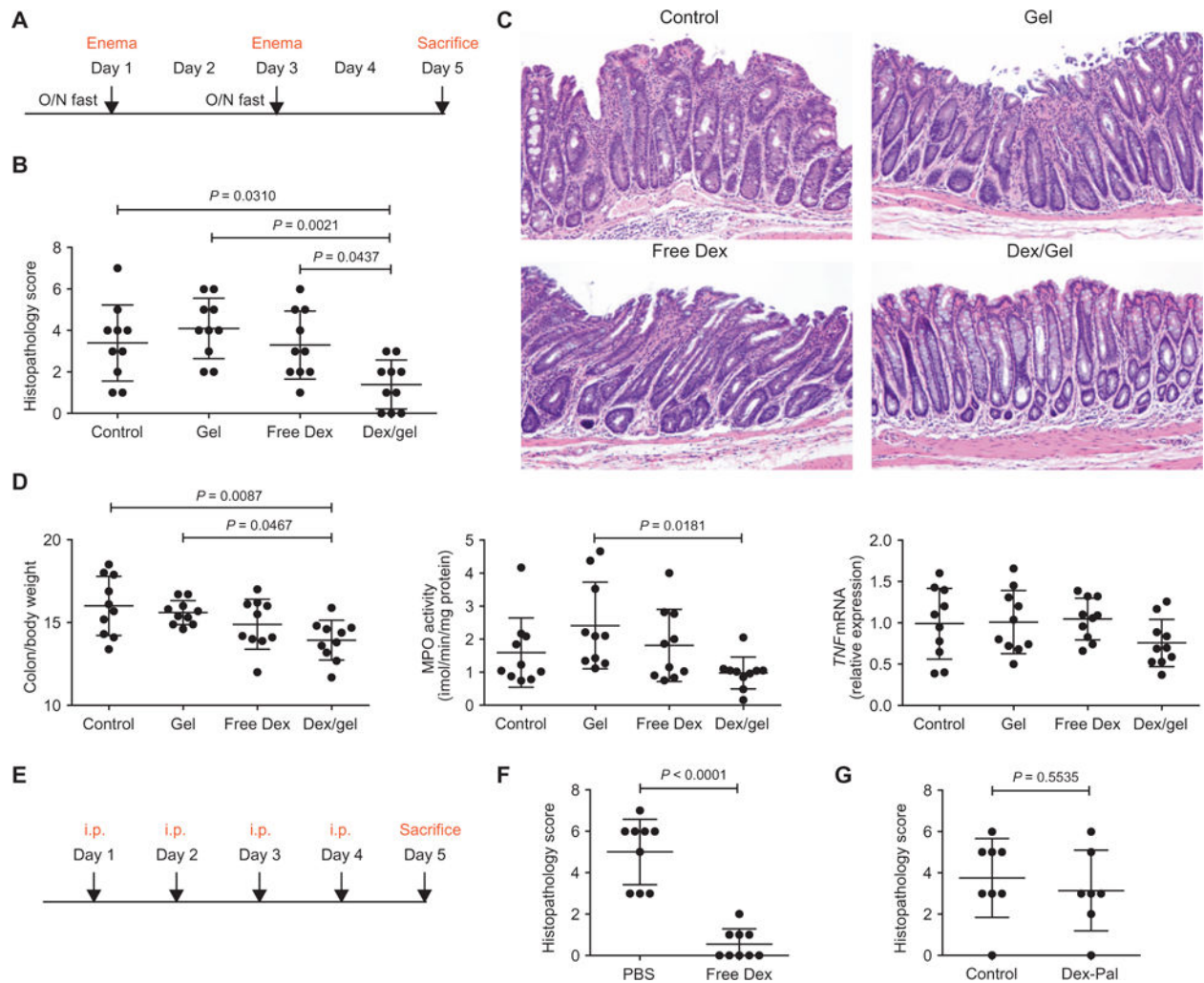


Fig. 4. Drug delivery via IT-hydrogel enema improves therapeutic efficacy when dosed every other day

(A) Colitic TRUC mice received enemas on days 1 and 3 after overnight (O/N) fasts; animals were sacrificed for analysis on day 5. (B) Histopathology scores after treatment with enemas of IT-hydrogel (Gel), free Dex, or Dex-loaded IT-hydrogel (Dex/gel, 70 μ g of Dex equivalent per dose in both groups). Control mice received no treatment. Data are means \pm SD ($n=10$ mice per group). $P=0.0029$ by one-way ANOVA; comparison of individual groups by Tukey post hoc test. (C) Representative hematoxylin and eosin (H&E) histology images of the experimental groups in (B). (D) Colon weight, MPO activity, and TNF mRNA levels in the distal colon measured in a second independent experiment. Data are means \pm SD ($n=10$ mice per group); P values were determined by one-way ANOVA with Tukey post hoc test. (E) TRUC mice received four daily intraperitoneal (i.p.) injections of free Dex (Dex-21 phosphate, 70 μ g of Dex equivalent per dose) or PBS; animals were sacrificed on day 5. (F) Histopathology scores for mice in (E) ($n=9$ mice per group). (G) Histopathology scores for TRUC mice treated with two enemas of Dex-Pal (70 μ g of Dex equivalent per dose) in vehicle (5% ethanol + 5% Tween 80) or vehicle only (Control) ($n=8$ mice per

group) using the dosing regimen described in (A). Data in (F) and (G) are means \pm SD; *P* values were determined by Student's *t* test.

Author Manuscript

Author Manuscript

Author Manuscript

Author Manuscript

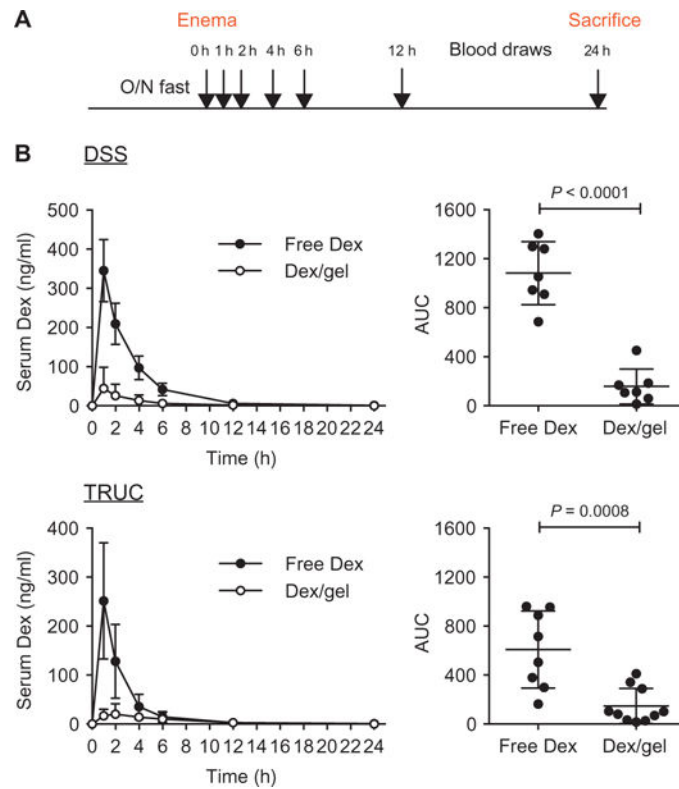


Fig. 5. Drug delivery via IT-hydrogel enema reduces systemic drug exposure

(A) Experimental design for the pharmacokinetic study. Colitic mice received a single enema of either free Dex or Dex-loaded IT-hydrogel (containing 70 μg of Dex equivalent) at 0 hour after an overnight fast. The serum Dex concentration was determined at 1, 2, 4, 6, 12, and 24 hours after enema, and the area under the curve (AUC) was calculated. (B) Results of the pharmacokinetic experiment described in (A) for WT mice with or without DSS-induced colitis and for TRUC mice compared with *Rag2*^{-/-} controls. Data are means \pm SD ($n = 7$ to 10 mice per group); P values were determined by Student's t test.

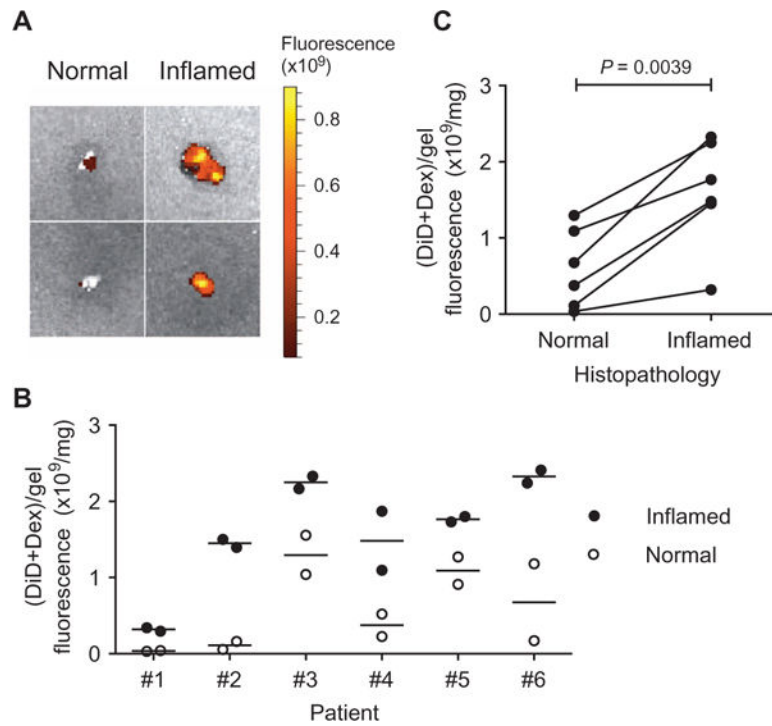


Fig. 6. IT-hydrogel preferentially adheres to inflamed human colon mucosa

(A) Representative IVIS image of duplicate samples from endoscopically normal and inflamed sites after incubation with (DiD + Dex)/gel. (B) Fluorescence intensity values for individual patient biopsy samples from histologically normal or inflamed locations. Values were normalized by tissue dry weight; data are means of duplicate samples. (C) Paired fluorescence intensity values for the patients in (B). Lines connected the paired means of duplicate samples for individual patients ($n = 6$). The P value was determined by paired t test.